


ORIGINAL RESEARCH

Pericoronary Fat Attenuation Index Is Associated With Vulnerable Plaque Components and Local Immune-Inflammatory Activation in Patients With Non-ST Elevation Acute Coronary Syndrome

Jia Teng Sun, MD, PhD*; Xin Cheng Sheng, MD*; Qi Feng, MD, PhD; Yan Yin, MD, PhD; Zheng Li, MD; Song Ding , MD, PhD; Jun Pu, MD, PhD

BACKGROUND: The pericoronary fat attenuation index (FAI) is assessed using standard coronary computed tomography angiography, and it has emerged as a novel imaging biomarker of coronary inflammation. The present study assessed whether increased pericoronary FAI values on coronary computed tomography angiography were associated with vulnerable plaque components and their intracellular cytokine levels in patients with non-ST elevation acute coronary syndrome.

METHODS AND RESULTS: A total of 195 lesions in 130 patients with non-ST elevation acute coronary syndrome were prospectively included. Lesion-specific pericoronary FAI, plaque components and other plaque features were evaluated by coronary computed tomography angiography. Local T cell subsets and their intracellular cytokine levels were detected by flow cytometry. Lesions with pericoronary FAI values >-70.1 Hounsfield units exhibited spotty calcification (43.1% versus 25.0%, $P=0.015$) and low-attenuation plaques (17.6% versus 4.2%, $P=0.016$) more frequently than lesions with lower pericoronary FAI values. Further quantitative plaque compositional analysis showed that increased necrotic core volume (Pearson's $r=0.324$, $P<0.001$) and fibrofatty volume (Pearson's $r=0.270$, $P<0.001$) were positively associated with the pericoronary FAI, and fibrous volume (Pearson's $r=-0.333$, $P<0.001$) showed a negative association. An increasing proinflammatory intracellular cytokine profile was found in lesions with higher pericoronary FAI values.

CONCLUSIONS: The pericoronary FAI may be a reliable indicator of local immune-inflammatory response activation, which is closely related to plaque vulnerability.

REGISTRATION: URL: <https://www.clinicaltrials.gov>; Unique identifier: NCT04792047.

Key Words: coronary computed tomography angiography ■ non-ST elevation acute coronary syndromes ■ pericoronary fat attenuation index ■ vulnerable plaque

Plaque vulnerability is causally related to acute coronary syndrome (ACS) development.¹ Long-term activation of the immune-inflammatory response is a main driver of plaque vulnerability. Vulnerable

plaques reveal large amounts of activated macrophages and differentiated subsets of T cells, which produce various proinflammatory and chemotactic cytokines.² Early identification of vulnerable plaques

Correspondence to: Song Ding, MD, PhD, Division of Cardiology, Renji Hospital, Shanghai Jiao Tong University School of Medicine, 160 Pujian Road, Shanghai 200127, China. E-mail: pujun_310@hotmail.com. Jun Pu, MD, PhD, Division of Cardiology, Renji Hospital, Shanghai Jiao Tong University School of Medicine, 160 Pujian Road, Shanghai 200127, China. E-mail: pujun_310@hotmail.com

†J. T. Sun and X. C. Sheng contributed equally.

Supplemental Material for this article is available at <https://www.ahajournals.org/doi/suppl/10.1161/JAHA.121.022879>

For Sources of Funding and Disclosures, see page 9.

© 2022 The Authors. Published on behalf of the American Heart Association, Inc., by Wiley. This is an open access article under the terms of the Creative Commons Attribution-NonCommercial-NoDerivs License, which permits use and distribution in any medium, provided the original work is properly cited, the use is non-commercial and no modifications or adaptations are made.

JAHA is available at: www.ahajournals.org/journal/jaha

CLINICAL PERSPECTIVE

What Is New?

- Lesions with high pericoronary fat attenuation index (FAI) values exhibited qualitative vulnerable plaque characteristics more frequently than lesions with lower FAI values in patients with non-ST elevation acute coronary syndrome.
- Increased necrotic core volume and fibrofatty volume were positively associated with the pericoronary FAI, while fibrous volume showed a negative association.
- An increasing pro-inflammatory cytokine profile were found in lesions with higher pericoronary FAI values.

What Are the Clinical Implications?

- Quantitative assessment of pericoronary FAI may help identify vulnerable plaque characteristics with increased local immune-inflammatory activation.

Nonstandard Abbreviations and Acronyms

FAI	fat attenuation index
HU	Hounsfield unit
ROI	region of interest

using an optimal imaging method is a field of increasing interest.^{3,4} However, further detection of coronary inflammation remains challenging, and standard invasive imaging methods, such as intravascular ultrasound (IVUS) and optical coherence tomography (OCT), limit visualization of the entire coronary tree and comprehensive assessment of the inflammatory burden of target lesions.^{5,6}

Coronary computed tomography angiography (CCTA) allows a detailed evaluation of the coronary wall anatomy and accurate classification of vulnerable plaque burden and morphology.⁷ A recent landmark study showed that CCTA detected coronary inflammation via quantification of the CT fat attenuation index (FAI).⁸ Local coronary inflammation contributes to a shift in perivascular adipose tissue composition from the lipid to aqueous phase adjacent to the inflamed coronary artery wall, which correlated with a gradient in the attenuation of perivascular adipose tissue captured using CCTA.⁹ The CRISP-CT study also showed that a pericoronary FAI value ≥ -70.1 Hounsfield unit (HU) was a reliable indicator of increased cardiac mortality or all-cause mortality independent of traditional risk factors.¹⁰ Early small-scale observational studies indicated

that pericoronary FAI correlated with plaque attenuation.¹¹ However, insights into the relationship between the pericoronary FAI and comprehensive quantitative plaque components of patients with non-ST elevation ACS (NSTEMI-ACS) are scarce.

Therefore, we investigated the relationship between CCTA-based pericoronary inflammation and plaque morphology and components in a large population-based cohort of subjects with NSTEMI-ACS. We hypothesized that the pericoronary FAI would be a reliable indicator of coronary immune-inflammatory disorder and closely related to plaque vulnerability.

METHODS

The authors declare that all supporting data are available within the article; further inquiries can be directed to the corresponding author(s).

Study Population

The Institutional Review Board of Renji Hospital approved this study, and all subjects provided written informed consent. Patients eligible for enrollment had ischemic symptoms and presented with ST depression ≥ 0.1 mV or elevated troponin levels. Patients with NSTEMI-ACS who needed an immediate (<2 hours) or early invasive strategy (<24 hours) according to guidelines were excluded, including patients who presented with hemodynamic instability or cardiogenic shock, life-threatening arrhythmias or cardiac arrest, mechanical complications, acute heart failure, dynamic ST or T wave changes, and a GRACE (Global Registry of Acute Coronary Events) score >140 .¹² Subjects with a previous history of coronary artery bypass graft surgery or percutaneous coronary intervention (PCI), immune system disorder, tumors, acute/chronic infection, atrial fibrillation, end-stage renal failure, iodine-containing contrast medium allergy, or statin use within 3 months were also excluded. Between January 2019 and January 2020, a total of 184 NSTEMI-ACS (non-ST-elevation myocardial infarction or unstable angina) patients aged 18 to 75 years who underwent CCTA were prospectively enrolled. After CCTA, we also excluded patients with no significant ($\geq 50\%$) stenosis in major epicardial vessels ($n=32$) and patients who refused subsequent angiography ($n=4$). Among the 148 remaining patients who received angiography, participants with total obstruction of major epicardial vessels ($n=6$), insufficient image quality for FAI and QAngioCT analysis ($n=10$), and a lack of blood samples ($n=2$) were excluded. A total of 130 patients with 195 lesions were ultimately included in our study for image analysis (Figure 1). The baseline features and cardiovascular risk factors for the study subjects were documented.

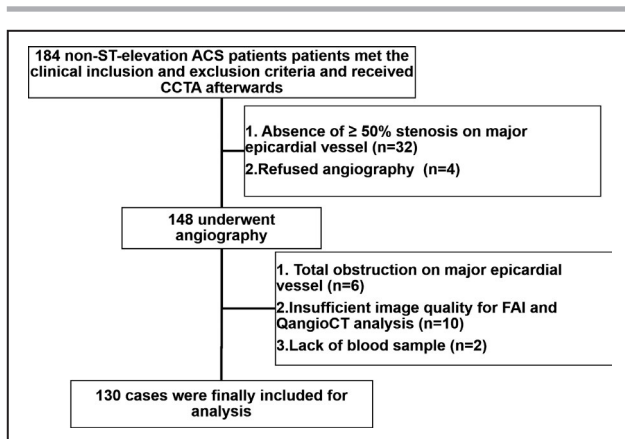


Figure 1. Flowchart of patient enrollment.

ACS indicates acute coronary syndrome; CCTA, coronary computed tomography angiography; and FAI, fat attenuation index.

Flow Cytometry

For quantification of the local T cell subset and immune-inflammatory mediators, 20 mL of blood was collected from the coronary artery using an aspiration thrombectomy catheter immediately after the diagnostic angiogram but before the intervention.^{13,14} For patients with multivessel coronary artery disease, the coronary blood sampling of each culprit vessel was collected separately for flow cytometry detection. T cell subsets and cytokine levels were detected using flow cytometry. Briefly, to quantify mature T, B, and NK lymphocyte populations and CD4+ and CD8+ T cell subsets in whole blood, BD Multitest™ four-color reagents were used for flow cytometry (BD FACSCalibur). The activated T cells were tested using BD Multitest™ reagents, including monoclonal antibodies (CD3/CD4/CD8/CD38/CD25/HLA-DR), and flow cytometry (BD FACSCanto). The percentage of Treg cells was detected using a BD Pharmingen™ FoxP3 Staining Kit and flow cytometry (BD FACSCanto). The quantification of cytokines was performed using BD™ Cytometric Bead Array (CBA) kits and flow cytometry (BD FACSCanto II).

CCTA Protocol and Plaque Analysis

All lesions with a stenosis of $\geq 50\%$ underwent quantitative analysis. CCTA examinations were performed using a 320-detector system (Aquilion ONE, Toshiba Medical Systems, Otawara, Japan). To achieve optimal imaging quality, oral metoprolol was administered before the CT scan to patients with heart rate >75 beats/min. The tube voltage and current for each patient were determined using the Toshiba integrated dose reduction technique (SureExposure 3D). ECGs were used for retrospective gating to eliminate interference by motions. The reconstruction of imaging data was 0.5-mm slice thickness and 0.25-mm reconstruction interval.

The plaques were assessed using original axial images, multiplanar reformation and cross-sectional reconstruction. Coronary plaque characteristics were analyzed across each of the main coronary arteries using a commercialized software package (Qangio CT, Medis, The Netherlands), which allowed fully automatic, quantitative assessment of plaque constitution and stenosis severity. Volumetric characterization of the plaque characteristics focused on the entire plaque volume under 3-dimensional (3D) reconstruction, and the cross-sectional characterization focused on the level of the minimal lumen area. We traced and analyzed lesions with a stenosis of $\geq 50\%$ in the proximal and middle segments of all 3 major coronary vessels. When a major coronary vessel presented with separate lesions, the more severely diseased lesion was evaluated. As for diffused coronary lesions, we analyzed the segment from the proximal normal segment to distal normal segment across the lesion. For the plaque constitution analysis, the following HU cut-off values used for classification: -30 to 75 for the necrotic core; 76 – 130 for fibrofatty plaques; 131 – 350 for fibrous plaques; and >351 for dense calcified plaques. Vulnerable plaque features were defined according to previous studies: low-attenuation plaque, mean CT number <30 HU; positive remodeling, remodeling index, >1.1 ; spotty calcification (SC), intraplaque calcification ≤ 3 mm; and napkin-ring sign, low intraplaque attenuation surrounded by a high attenuation rim. An example of Left Anterior Descending artery plaque quantitative analysis is shown in Figure 2A through 2C. Two experienced observers who were blinded to the clinical data assessed the presence of vulnerable plaques in each lesion.

Pericoronary FAI Analysis

As described by Antonopoulos et al,⁸ the pericoronary FAI was defined as the mean CT attenuation of the pericoronary adipose tissue (-190 to -30 HU). Lesion-based FAI was measured around the lesion segment of all 3 major epicardial coronary vessels located within a radial distance from the outer vessel wall equal to the diameter of the respective vessel. We did not have their artificial intelligence-based segmentation algorithm, therefore we segmented the pericoronary adipose tissue manually with MITK software (<https://www.mitk.org/>, v2018.04.2). We first drew lesion segments of the vessels and the plaques around the vessels as an initial region of interest (ROI) on 3D CCTA images then dilated the initial ROI with the size of the mean diameter of the vessel to obtain a dilated ROI using morphological operation “Dilatation” in Segmentation module. The mismatch region between the dilated ROI and initial ROI was segmented using the Boolean operation “Difference” in Segmentation Utilities module and defined as the

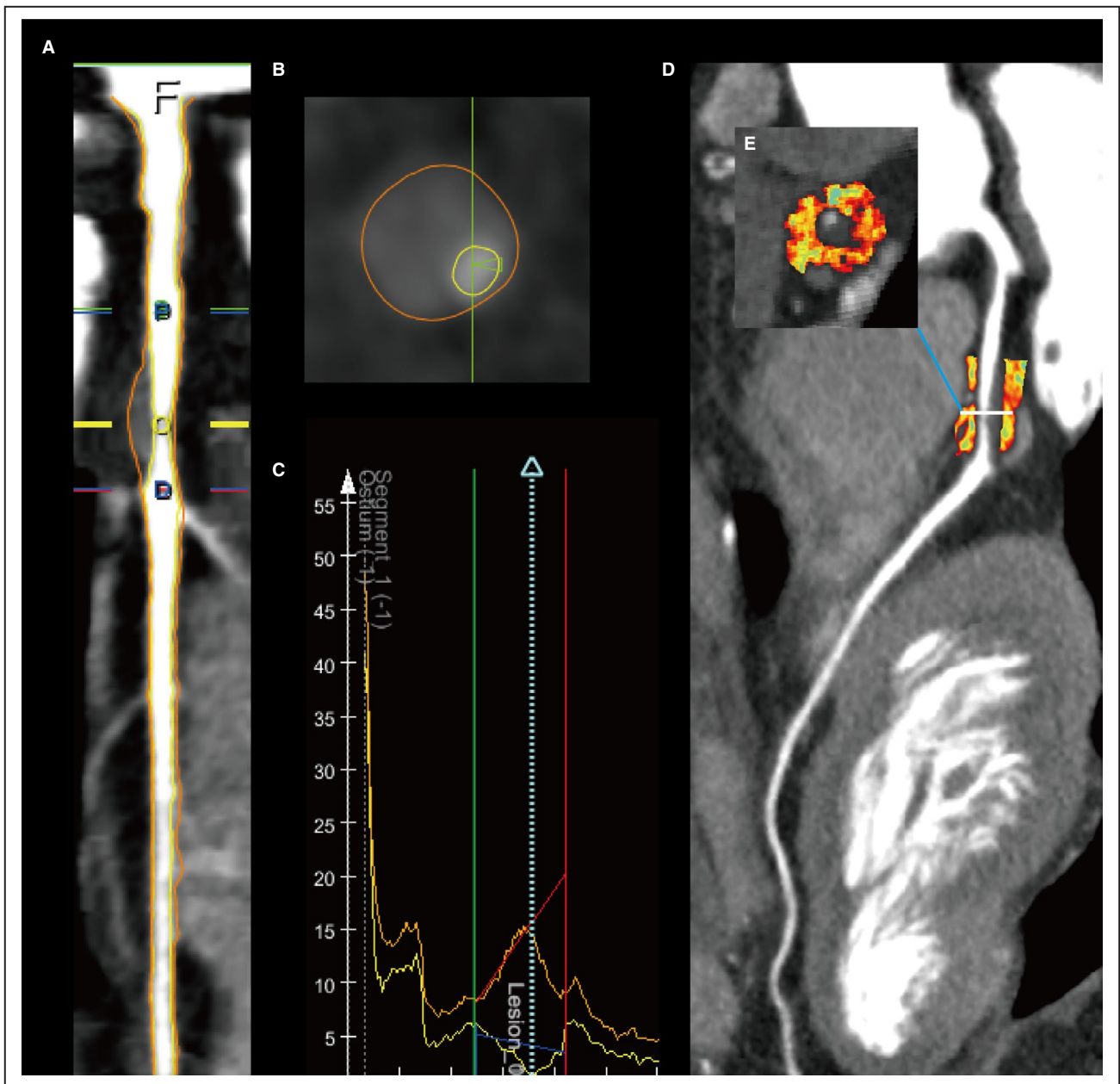


Figure 2. Example of coronary plaque quantitative analysis and pericoronary FAI phenotyping of a lesion in the proximal LAD artery segment.

A, Longitudinal straightened multiplanar reconstruction, where “O” is the point of minimum lumen area. **B**, Cross-sectional view at the point of minimum lumen area. **C**, Graph of lumen and vessel area as a function of vessel length. **D**, Straightened view of FAI phenotyping. **E**, Cross-section view of FAI phenotyping. FAI indicates fat attenuation index; and LAD, left anterior descending.

perivessel ROI, which was subsequently filtered using -190 HU to -30 HU intervals to remove the nonfatty tissue and obtain the final lesion-based perivessel fat ROI. The left main coronary artery was not analyzed because it is of variable length. Representative images of pericoronary FAI detection are shown in Figure 2D and 2E. Two experienced cardiovascular radiologists who were blinded to the results of other tests measured the values of the lesion-based FAI.

Statistical Analysis

Data are presented as the means \pm standard deviation when normally distributed or as the medians and interquartile range (IQR) when not normally distributed for continuous variables and as percentages for categorical variables. Continuous variables were compared using unpaired Student’s *t* tests for normally distributed data. Otherwise, the Mann-Whitney U test or Kruskal-Wallis test was performed. The chi-squared test was

used to compare categorical variables. Pearson correlational analysis was performed to detect the correlations between the pericoronary FAI and other variables as appropriate. The results were considered statistically significant when a two-sided *P* value was <0.05. Furthermore, threshold level of significance for differences among groups were adjusted for multiple comparisons by Bonferroni's correction. The differences were statistically significant when the observed *P* values were less than the specified significance level (α) divided by the number of tests (K)=0.05/*n*. Statistical analyses were performed using SPSS (IBM SPSS 23.0, SPSS Inc.).

RESULTS

Clinical Characteristics

A total of 195 lesions from 130 patients were analyzed in our study. The median population age was 65 years, and the male prevalence was 66.9% (87 of 130 patients). The comorbidities and laboratory data are summarized in Table 1.

Pericoronary FAI Values and CCTA Features

The distribution of targeted lesions among the three major coronary arteries did not differ between the 2 groups. The prevalence of vulnerable features was significantly increased in lesions with pericoronary FAI values ≥ -70.1 (54.9% versus 38.2%, *P*=0.038). Spotty calcifications (43.1% versus 25.0%, *P*=0.015) and low-attenuation plaques (17.6% versus 4.2%, *P*=0.016) were more frequently observed in lesions with high pericoronary FAI values. No significant differences were noted in the rate of positive remodeling or napkin signs between the 2 groups (Table 2). Overall, the

FAI values were higher in vulnerable lesions compared with non-vulnerable lesions (-72.9 [-81.8 , -64.7] versus -78.8 [-87.7 , -68.0] HU, *P*=0.003) (Figure S1).

The plaque burden including whole plaque volume, mean plaque burden and maximal plaque thickness were significantly increased in lesions with increased FAI values. Examinations of specific plaque components showed that lesions with pericoronary FAI values > -70.1 HU had significantly higher necrotic core volume (54.22 [36.41, 84.76] versus 19.86 [9.01, 68.46] mm³; *P*=0.002) than lesions with pericoronary FAI values < -70.1 HU at the level of the entire lesion volumetric but did not differ significantly in fibrofatty volume, dense calcium volume or fibrous volume (Table 3). However, there was no significant difference in plaque components or burden at the level of minimum lumen area between the different FAI groups (Table 4). Positive correlations were observed between the pericoronary FAI and mean plaque burden (Pearson's *r*=0.329, *P*<0.001), necrotic core volume (Pearson's *r*=0.324, *P*<0.001) and fibrous fatty volume (Pearson's *r*=0.270, *P*<0.001) at the level of the entire lesion volumetric. Our study also revealed a negative relationship between the pericoronary FAI and fibrous volume (Pearson's *r*=-0.333, *P*<0.001) (Figure 3).

Pericoronary FAI and Local Immune-Inflammatory Activation

Proinflammatory cytokine, IL-17 (3.44 [1.27, 6.35] versus 1.66 [0.76, 3.92] pg/mL; *P*=0.001) was remarkably elevated in lesions with higher pericoronary FAI values, and the anti-inflammatory cytokine IL-10 (2.29 [1.64, 3.11] versus 2.85 [2.33, 3.34] pg/mL; *P*=0.005) showed the opposite trend. Lesions with higher perivascular FAI values tended to exhibit decreased local Treg

Table 1. Clinical Characteristics of Study Patients

Patients number, n	130
Lesion number, n	195
Baseline characteristic	
Age, y	65.00 (61.00, 71.00)
Sex, M/F	87/43
BMI, kg/m ²	24.45 (22.66, 26.53)
Hypertension, n (%)	85 (65.4)
DM, n (%)	38 (29.2)
Hyperlipidemia (%)	40 (30.7)
Biochemical assessment	
CRP, mg/L	1.36 (0.61, 3.80)
ALT, U/L	19.50 (14.00, 28.25)
Creatinine, μ mol/L	71.50 (62.00, 82.00)

ALT indicates alanine aminotransferase; BMI, body mass index; CRP, C-response protein; DM, diabetes; and M/F, male/female.

Table 2. Coronary Arteries Distribution and Prevalence of Vulnerable Features in Lesions With High or Low Pericoronary FAI Values

	FAI ≥ -70.1 HU (n=51)	FAI<-70.1 HU (n=144)	<i>P</i> value
Coronary arteries			0.423
LAD, n (%)	23 (45.1)	72 (50.0)	
LCX, n (%)	14 (27.5)	27 (18.8)	
RCA, n (%)	14 (27.5)	45 (31.3)	
Vulnerable plaque prevalence	28 (54.9)	55 (38.2)	0.038
Spotty calcification, n (%)	22 (43.1)	36 (25.0)	0.015
Low-attenuation plaque, n (%)	9 (17.6)	9 (4.2)	0.016
Positive remodeling, n (%)	8 (15.7)	16 (11.1)	0.393
Napkin-ring sign, n (%)	2 (3.9)	5 (3.5)	0.882

CCTA indicates coronary computed tomographic angiography; FAI, fat attenuation index; HU, Hounsfield unit; LAD, Left Anterior Descending; LCX, Left Circumflex; and RCA, Right Coronary.

Table 3. Plaque Components With High or Low Pericoronary FAI Values at the Level of Entire Lesion Volumetric

	FAI \geq -70.1 HU (n=51)	FAI<70.1 HU (n=144)	P value
Plaque volume, mm ³	229.35 (161.01, 310.94)	142.02 (60.28, 255.06)	0.002*
Mean plaque burden, %	64.82 \pm 10.77	58.49 \pm 9.90	<0.001*
Maximal plaque thickness, mm	2.52 \pm 0.74	2.18 \pm 0.70	0.005*
Absolute volume of plaque components			
Fibrous volume, mm ³	97.10 (54.31, 139.34)	64.76 (26.81, 128.96)	0.067
Fibrofatty volume, mm ³	35.85 (24.81, 51.42)	24.81 (9.24, 47.91)	0.053
Necrotic core volume, mm ³	54.22 (36.41, 84.76)	19.86 (9.01, 68.46)	0.002†
Dense calcified volume, mm ³	1.99 (0.60, 16.14)	2.82 (0.67, 8.28)	0.084
Percentage of plaque components			
Fibrous volume, %	49.23 (30.15, 60.86)	50.68 (36.42, 68.68)	0.041
Fibrofatty volume, %	18.37 (12.22, 20.69)	17.33 (11.75, 21.41)	0.370
Necrotic core volume, %	28.12 (15.75, 45.92)	24.37 (8.43, 38.74)	0.019
Dense calcified volume, %	1.23 (0.43, 9.74)	1.19 (0.31, 5.73)	0.157

FAI indicates fat attenuation index; and HU, Hounsfield unit.

* $P < 0.0167$ (0.05/3).

† $P < 0.0125$ (0.05/4).

numbers, however not reached statistically significant (Table 5).

DISCUSSION

Our study demonstrated the following main findings. First, we showed that lesions with high pericoronary FAI values exhibited qualitative vulnerable plaque characteristics more frequently than lesions with lower FAI values in patients with NSTEMI-ACS. Second, quantitative plaque component assessment further demonstrated that higher necrotic core volume and fibrous fatty volume were positively associated with increased pericoronary FAI values, and fibrous volume had the opposite effect. Third, we described, for the first time, that the presence of lesions with higher pericoronary FAI values was associated with a proinflammatory

cytokine profile. These results support the use of pericoronary FAI as a reliable indicator of coronary immune-inflammatory activation and is closely related to plaque vulnerability.

Vascular inflammation and immune activation are key regulators of lipid core formation and fibrous cap thickness, which were proposed as determinants of plaque vulnerability.^{15,16} Antonopoulos et al first reported the detection and quantification of coronary inflammation using the FAI as a noninvasive imaging biomarker and the routine CCTA method.⁸ This study followed an observational study by Goller et al who demonstrated that the pericoronary FAI was substantially elevated around culprit lesions compared to non-culprit lesions in the presence of ACS.¹¹ Our study extended the established correlation between pericoronary FAI and coronary plaque characteristics by demonstrating

Table 4. Plaque Components With High or Low Pericoronary FAI Values at the Level of Minimal Lumen Area

	FAI \geq -70.1 HU (n=51)	FAI<70.1 HU (n=144)	P value
Plaque burden, %	80.54 (73.52, 86.75)	81.16 (72.74, 88.79)	0.649
Maximal plaque thickness, mm	2.06 \pm 0.62	1.98 \pm 0.62	0.490
Absolute area of plaque components			
Fibrous area, mm ²	3.12 (1.16, 5.95)	3.46 (1.18, 6.67)	0.276
Fibrofatty area, mm ²	1.79 (0.77, 3.02)	1.88 (1.00, 3.16)	0.157
Necrotic core area, mm ²	3.94 (0.80, 5.95)	3.41 (0.73, 7.15)	0.246
Dense calcified area, mm ²	0.12 (0.06, 1.01)	0.11 (0.04, 0.95)	0.675
Percentage of plaque components			
Fibrous area, %	38.46 (9.37, 59.29)	31.17 (11.35, 58.79)	0.829
Fibrofatty area, %	16.43 (10.29, 26.68)	16.24 (11.94, 26.82)	0.652
Necrotic core area, %	33.38 (10.85, 58.60)	34.39 (6.85, 61.24)	0.545
Dense calcified area, %	0.17 (0.05, 0.94)	0.16 (0.04, 0.93)	0.683

FAI indicates fat attenuation index; and HU, Hounsfield unit.

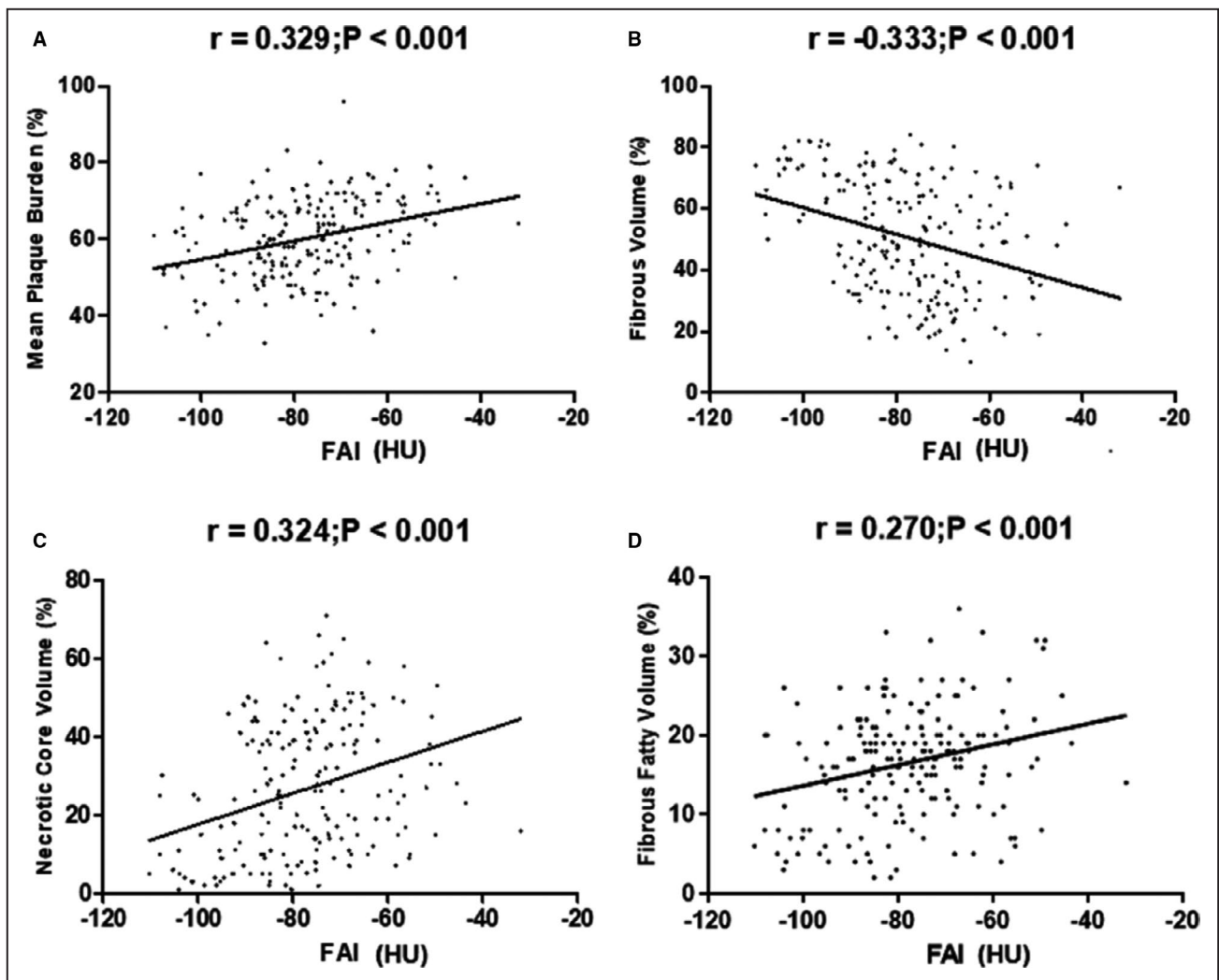


Figure 3. Correlation between FAI values and mean plaque burden (A), fibrous volume (B), necrotic core volume (C), fibrous fatty volume (D).

FAI indicates fat attenuation index; and HU, Hounsfield unit.

that pericoronary FAI correlated with vulnerable plaque components detected by CCTA in patients with ACS at low risk. We provided evidence that lesions with a pericoronary FAI cutoff of -70.1 HU or higher (an optimum cutoff value for predicting increased cardiac mortality established in a previous study¹⁰) exhibited an increased frequency of plaque vulnerability, including low-attenuation plaque and spotty calcification. Quantitative measurement of plaque composition using Qangio CT was also used to examine the association between FAI and vulnerable plaque components. To the best of our knowledge, this study is the first study to report a significant positive correlation between the FAI and necrotic core volume and a negative relationship between the FAI and fibrous volume in ACS lesions. These plaque compositional features are also representative of plaque vulnerability because our early research using virtual histology (VH)-IVUS

showed that a large necrotic core was more frequently observed in the culprit lesions of patients with ACS than in stable angina.¹⁷ Therefore, the correlation between the FAI and plaque components supports the link between vascular inflammation and plaque vulnerability at a noninvasive imaging level. These findings are consistent with the causal relationship of increased inflammatory burden with low-attenuation plaque and microcalcification formation that was clinically and pathologically confirmed in previous investigators.^{18–20}

In addition to coronary atherosclerotic plaque features, overall atherosclerotic disease burden was another powerful indicator of future adverse cardiac events.²¹ The plaque volume was significantly increased in lesions with increased FAI values. Notably, the plaque burdens and compositional features at the minimum lumen area between different FAI groups were comparable. This result is well explained by the

Table 5. T Cell Subsets and Cytokines Levels of Lesions With High or Low Pericoronary FAI Values

	FAI \geq -70.1 HU (n=51)	FAI<70.1 HU (n=144)	P value
T cell subsets			
Treg, %	8.13 (7.01, 11.58)	10.92 (9.17, 13.03)	0.013
B lymphocytes (CD3-CD19+) %	11.73 (8.27, 13.41)	11.22 (9.47, 14.53)	0.688
T lymphocytes (CD3+) %	69.80 (61.52, 73.07)	70.05 (63.83, 74.42)	0.934
Th lymphocytes (CD3+CD4+) %	39.57 (37.11, 46.06)	42.30 (36.73, 47.58)	0.628
Ts lymphocytes (CD3+CD8+) %	24.26 (20.12, 31.18)	26.15 (19.57, 30.63)	0.870
CD4/CD8	1.53 (1.29, 2.37)	1.63 (1.25, 2.36)	0.833
Natural killer cell %	1.59 (1.20, 1.87)	1.69 (1.25, 2.07)	0.678
Cytokine levels			
IL-2, pg/mL	1.53 (1.36, 1.85)	1.23 (0.78, 1.84)	0.014
IL-4, pg/mL	1.57 (0.82, 1.93)	1.05 (0.42, 2.14)	0.397
IL-6, pg/mL	6.86 (4.68, 8.67)	4.42 (3.34, 6.46)	0.027
IL-10, pg/mL	2.29 (1.64, 3.11)	2.85 (2.33, 3.34)	0.005*
IL-17, pg/mL	3.44 (1.27, 6.35)	1.66 (0.76, 3.92)	0.001*
TNF- α , pg/mL	1.35 (0.96, 1.85)	1.15 (0.73, 2.03)	0.439

FAI indicates fat attenuation; HU, Hounsfield unit; and IL, interleukin.

* $P < 0.0083$ (0.05/6).

fact that the FAI represented the 3D attenuation within perivascular adipose tissue space rather than a transverse quantification.

Vulnerable atherosclerotic lesions skew immune-inflammatory status activation, which is characterized by increased Th17 and decreased Treg cells.^{22,23} Activation of Th17 cells in atherosclerotic lesions participates in atherosclerosis via the production of high concentrations of IL-17 and, to a lesser extent, IL-6 and tumor necrosis factor alpha (TNF α).²⁴ The enhanced inflammatory status in vulnerable plaques and inflammatory cytokines exerted inhibitory effects on preadipocyte differentiation, which was revealed in an in vitro study.⁸ We next tested the hypothesis that the pericoronary FAI value was associated with in vivo local T cell subsets and their intracellular cytokine levels. Our study first established an association between higher local expression of IL-17 and increased FAI values in vivo. In line with our observations, Elnabawi et al recently showed that anti-IL-17 treatment improved coronary inflammation at a 1-year follow-up.²⁵ Treg cells exert atheroprotective activities by secreting anti-inflammatory cytokines, such as IL-10.²⁶ A lower IL-10 concentration correlated with a higher plaque burden.²⁷ The present study observed that lesions with higher FAI values had decreased IL-10 level, which suggests a causal role for the TH17/Treg imbalance in the coronary inflammation burden. In addition, a previous report failed to show a positive correlation between serum hs-CRP (high-sensitivity C-reactive protein) levels and pericoronary FAI.²⁸ We hypothesized that pericoronary FAI was driven by local inflammatory stimuli from the lesion rather than systemic inflammatory disorders. Notably, the use of aspiration catheters in our

study allowed sampling at the site of coronary stenosis lesions. Cytokines at the lesion site were better indicators of atherosclerosis-associated inflammation than their counterparts in peripheral blood.²⁹ Consequently, measurement of circulating CRP, which is a downstream biomarker of systemic inflammation, lacks specificity for coronary inflammation.

Taken together, our findings support the hypothesis that the FAI is a sensitive imaging biomarker of the inflammatory burden of coronary vessels and the imbalance of local pro- and anti-inflammatory mediators.

CONCLUSION

The current study extends the findings of other studies to indicate that quantitative assessment of pericoronary FAI helps identify vulnerable plaque characteristics with increased local immune-inflammatory activation. Therefore, FAI evaluation, as a noninvasive imaging analysis, further supports the immune-inflammation hypothesis for vulnerable plaque formation that evolved from histological evidence.

Limitations

There are several limitations to our work. First, the study was observational and performed at a single center. Second, although the pericoronary FAI and plaque features were correlated, we lacked follow-up data and a sufficient number of patients to demonstrate the predictive value of this imaging marker for plaque instability and subsequent adverse cardiac events. Third, lesions under 50% stenosis were excluded from our study. Therefore, future studies will

need to assess whether coronary FAI identifies cases with a high risk of events before significant stenosis. Fourth, the 2020 ESC guidelines for the management of ACS recommendation¹² recommend coronary CTA as an alternative to invasive angiography to exclude ACS when there is a low-to-intermediate likelihood of CAD. STEMI and in high-risk ACS patients who require an early invasive strategy were excluded in the present study although these patients might present enhanced inflammatory burden. Finally, not all strong inflammatory biomarkers such as IL-1 β with available biologic therapy were included in our study. The translational value of FAI in coronary inflammation treatment needs to be further confirmed.

ARTICLE INFORMATION

Received June 14, 2021; accepted November 22, 2021.

Affiliations

Department of Cardiology (J.T.S., X.C.S., Z.L., S.D., J.P.) and Department of Radiology (Q.F., Y.Y.), Ren Ji Hospital, Shanghai Jiao Tong University School of Medicine, Shanghai, China.

Acknowledgments

The authors acknowledge the core laboratory (CardHemo, Med-X Research Institute, Shanghai Jiao Tong University, Shanghai, China) for guidance and quality control of QangioCT analyses and acknowledge Dr Shao Feng Duan for guidance and quality control of pericoronary FAI analyses.

Sources of Funding

This work was supported by grants from the National Natural Science Foundation of China (82070477, 81800223), Shanghai Jiao Tong University School of Medicine (DLY201804), Shanghai Science and Technology Committee (19ZR1430400), Shanghai ShenKang Hospital Development Center (SHDC12019X12), Shanghai Sailing Program (18YF1413500), Shanghai Municipal Key Clinical Specialty (shslczdk06204).

Disclosures

None.

Supplementary Material

Figure S1

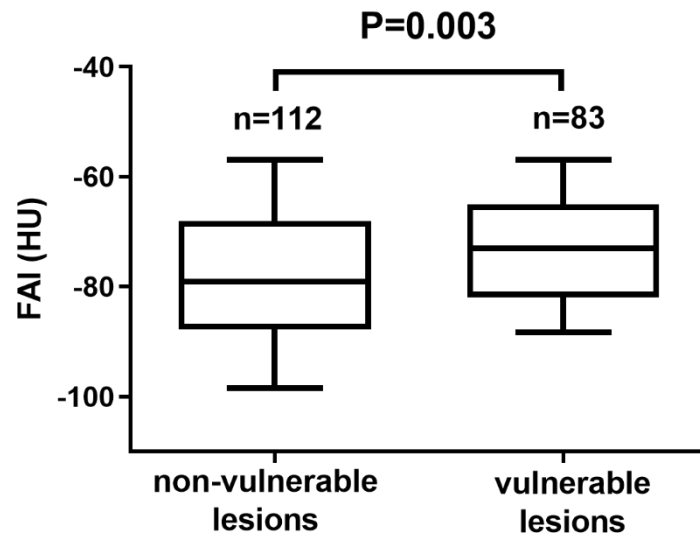
REFERENCES

- Motoyama S, Sarai M, Harigaya H, Anno H, Inoue K, Hara T, Naruse H, Ishii J, Hishida H, Wong ND, et al. Computed tomographic angiography characteristics of atherosclerotic plaques subsequently resulting in acute coronary syndrome. *J Am Coll Cardiol*. 2009;54:49–57. doi: 10.1016/j.jacc.2009.02.068
- Fernandez DM, Rahman AH, Fernandez NF, Chudnovskiy A, Amir E-A, Amadori L, Khan NS, Wong CK, Shamailova R, Hill CA, et al. Single-cell immune landscape of human atherosclerotic plaques. *Nat Med*. 2019;25:1576–1588. doi: 10.1038/s41591-019-0590-4
- Toutouzias K, Benetos G, Karanasos A, Chatzizisis YS, Giannopoulos AA, Tousoulis D. Vulnerable plaque imaging: updates on new pathobiological mechanisms. *Eur Heart J*. 2015;36:3147–3154. doi: 10.1093/eurheartj/ehv508
- Otsuka F, Joner M, Prati F, Virmani R, Narula J. Clinical classification of plaque morphology in coronary disease. *Nat Rev Cardiol*. 2014;11:379–389. doi: 10.1038/nrcardio.2014.62
- Mushenkova NV, Summerhill VI, Zhang D, Romanenko EB, Grechko AV, Orekhov AN. Current advances in the diagnostic imaging of atherosclerosis: insights into the pathophysiology of vulnerable plaque. *Int J Mol Sci*. 2020;21. doi: 10.3390/ijms21082992
- Stone GW, Maehara A, Lansky AJ, de Bruyne B, Cristea E, Mintz GS, Mehran R, McPherson J, Farhat N, Marso SP, et al. A prospective natural-history study of coronary atherosclerosis. *New Engl J Med*. 2011;364:226–235. doi: 10.1056/NEJMoa1002358
- Andreini D, Magnoni M, Conte E, Masson S, Mushtaq S, Berti S, Canestrari M, Casolo G, Gabrielli D, Latini R, et al. Coronary plaque features on CTA can identify patients at increased risk of cardiovascular events. *JACC Cardiovasc Imaging*. 2020;13:1704–1717. doi: 10.1016/j.jcmg.2019.06.019
- Antonopoulos AS, Sanna F, Sabharwal N, Thomas S, Oikonomou EK, Herdman L, Margaritis M, Shirodaria C, Kampoli A-M, Akoumianakis I, et al. Detecting human coronary inflammation by imaging perivascular fat. *Sci Transl Med*. 2017;9. doi: 10.1126/scitranslmed.aal2658
- Antoniades C, Kotanidis CP, Berman DS. State-of-the-art review article. Atherosclerosis affecting fat: what can we learn by imaging perivascular adipose tissue? *J Cardiovasc Comput Tomogr*. 2019;13:288–296. doi: 10.1016/j.jcct.2019.03.006
- Oikonomou EK, Marwan M, Desai MY, Mancio J, Alashi A, Hutt Centeno E, Thomas S, Herdman L, Kotanidis CP, Thomas KE, et al. Non-invasive detection of coronary inflammation using computed tomography and prediction of residual cardiovascular risk (the CRISP CT study): a post-hoc analysis of prospective outcome data. *Lancet*. 2018;392:929–939. doi: 10.1016/S0140-6736(18)31114-0
- Goeller M, Achenbach S, Cadet S, Kwan AC, Commandeur F, Slomka PJ, Gransar H, Albrecht MH, Tamarappoo BK, Berman DS, et al. Pericoronary adipose tissue computed tomography attenuation and high-risk plaque characteristics in acute coronary syndrome compared with stable coronary artery disease. *JAMA Cardiol*. 2018;3:858–863. doi: 10.1001/jamacardio.2018.1997
- Collet J-P, Thiele H, Barbato E, Barthélémy O, Bauersachs J, Bhatt DL, Dendale P, Dorobantu M, Edvardsen T, Folliguet T, et al. 2020 ESC guidelines for the management of acute coronary syndromes in patients presenting without persistent ST-segment elevation. *Eur Heart J*. 2021;42:1289–1367. doi: 10.1093/eurheartj/ehaa575
- Mangold A, Ondracek AS, Hofbauer TM, Scherz T, Artner T, Panagiotides N, Beitzke D, Ruzicka G, Nistler S, Wohlschläger-Krenn E, et al. Culprit site extracellular DNA and microvascular obstruction in ST-elevation myocardial infarction. *Cardiovasc Res*. 2021;cvab217. doi: 10.1093/cvr/cvab217
- Leistner DM, Kränkel N, Meteva D, Abdelwahed YS, Seppelt C, Stähli BE, Rai H, Skurk C, Lauten A, Mochmann H-C, et al. Differential immunological signature at the culprit site distinguishes acute coronary syndrome with intact from acute coronary syndrome with ruptured fibrous cap: results from the prospective translational OPTICO-ACS study. *Eur Heart J*. 2020;41:3549–3560. doi: 10.1093/eurheartj/ehaa703
- Crea F, Libby P. Acute coronary syndromes: the way forward from mechanisms to precision treatment. *Circulation*. 2017;136:1155–1166. doi: 10.1161/CIRCULATIONAHA.117.029870
- Mangge H, Almer G. Immune-mediated inflammation in vulnerable atherosclerotic plaques. *Molecules (Basel, Switzerland)*. 2019;24:3072. doi: 10.3390/molecules24173072
- Pu J, Mintz GS, Brilakis ES, Banerjee S, Abdel-Karim A-R R, Maini B, Biro S, Lee J-B, Stone GW, Weisz G, et al. In vivo characterization of coronary plaques: novel findings from comparing greyscale and virtual histology intravascular ultrasound and near-infrared spectroscopy. *Eur Heart J*. 2012;33:372–383. doi: 10.1093/eurheartj/ehr387
- Nakahara T, Dweck MR, Narula N, Pisapia D, Narula J, Strauss HW. Coronary artery calcification: from mechanism to molecular imaging. *JACC Cardiovasc Imaging*. 2017;10:582–593. doi: 10.1016/j.jcmg.2017.03.005
- Tahara N, Kai H, Ishibashi M, Nakaura H, Kaida H, Baba K, Hayabuchi N, Imaizumi T. Simvastatin attenuates plaque inflammation: evaluation by fluorodeoxyglucose positron emission tomography. *J Am Coll Cardiol*. 2006;48:1825–1831. doi: 10.1016/j.jacc.2006.03.069
- Bäck M, Yurdagül A Jr, Tabas I, Öörni K, Kovanen PT. Inflammation and its resolution in atherosclerosis: mediators and therapeutic opportunities. *Nat Rev Cardiol*. 2019;16:389–406. doi: 10.1038/s41569-019-0169-2
- Schuurman A-S, Vroegindewey MM, Kardys I, Oemrawsingh RM, Garcia-Garcia HM, van Geuns R-J, Regar E, Van Mieghem NM, Ligthart J, Serruys PW, et al. Prognostic value of intravascular ultrasound in patients with coronary artery disease. *J Am Coll Cardiol*. 2018;72:2003–2011. doi: 10.1016/j.jacc.2018.08.2140
- Joly AL, Seitz C, Liu S, Kuznetsov NV, Gertow K, Westerberg LS, Paulsson-Berne G, Hansson GK, Andersson J. Alternative splicing of

- foxp3 controls regulatory T cell effector functions and is associated with human atherosclerotic plaque stability. *Circ Res*. 2018;122:1385–1394. doi: 10.1161/CIRCRESAHA.117.312340
23. George J, Schwartzberg S, Medvedovsky D, Jonas M, Charach G, Afek A, Shamiss A. Regulatory T cells and il-10 levels are reduced in patients with vulnerable coronary plaques. *Atherosclerosis*. 2012;222:519–523. doi: 10.1016/j.atherosclerosis.2012.03.016
24. Wolf D, Ley K. Immunity and inflammation in atherosclerosis. *Circ Res*. 2019;124:315–327. doi: 10.1161/CIRCRESAHA.118.313591
25. Elnabawi YA, Oikonomou EK, Dey AK, Mancio J, Rodante JA, Aksentijevich M, Choi H, Keel A, Erb-Alvarez J, Teague HL, et al. Association of biologic therapy with coronary inflammation in patients with psoriasis as assessed by perivascular fat attenuation index. *JAMA Cardiol*. 2019;4:885–891. doi: 10.1001/jamacardio.2019.2589
26. Pinderski Oslund LJ, Hedrick CC, Olvera T, Hagenbaugh A, Territo M, Berliner JA, Fyfe AI. Interleukin-10 blocks atherosclerotic events in vitro and in vivo. *Arterioscler Thromb Vasc Biol*. 1999;19:2847–2853. doi: 10.1161/01.ATV.19.12.2847
27. Battes LC, Cheng JM, Oemrawsingh RM, Boersma E, Garcia-Garcia HM, de Boer SPM, Buljubasic N, Mieghem NAV, Regar E, Geuns R-J, et al. Circulating cytokines in relation to the extent and composition of coronary atherosclerosis: results from the ATHEROREMO-IVUS study. *Atherosclerosis*. 2014;236:18–24. doi: 10.1016/j.atherosclerosis.2014.06.010
28. Dai X, Deng J, Yu M, Lu Z, Shen C, Zhang J. Perivascular fat attenuation index and high-risk plaque features evaluated by coronary CT angiography: relationship with serum inflammatory marker level. *Int J Cardiovasc Imaging*. 2020;36:723–730. doi: 10.1007/s10554-019-01758-8
29. Lluberas N, Trías N, Brugnini A, Mila R, Vignolo G, Trujillo P, Durán A, Grille S, Lluberas R, Lens D. Lymphocyte subpopulations in myocardial infarction: a comparison between peripheral and intracoronary blood. *SpringerPlus*. 2015;4:744. doi: 10.1186/s40064-015-1532-3

SUPPLEMENTAL MATERIAL

Figure S1. Comparison of FAI values in vulnerable and non-vulnerable lesions.



FAI: fat attenuation index.